

Theoretical analysis of quantum dynamics in one-dimensional lattices: Wannier-Stark description

Quentin Thommen,* Jean Claude Garreau,[†] and Véronique Zehnle[‡]

*Laboratoire de Physique des Lasers, Atomes et Molécules, Centre d'Etudes et de Recherches Laser et Applications,
Université des Sciences et Technologies de Lille, F-59655 Villeneuve d'Ascq Cedex, France[§]*

(Received 19 December 2001; published 22 April 2002)

This paper presents a formalism describing the dynamics of a quantum particle in a one-dimensional, tilted, time-dependent lattice. The description uses the Wannier-Stark states, which are localized in each site of the lattice, and provides a simple framework leading to fully analytical developments. Particular attention is devoted to the case of a time-dependent potential, which results in a rich variety of quantum coherent dynamics.

DOI: 10.1103/PhysRevA.65.053406

PACS number(s): 03.65.-w, 03.75.-b, 32.80.Lg, 32.80.Pj

I. INTRODUCTION

Quantum dynamics in a periodic lattice is one of the oldest problems of quantum mechanics, whose basis was settled by Bloch [1] and Zener [2], around 1930. Aimed at a description of the electron motion in crystalline lattices, this problem has been considered for about half a century as an academic one, because dissipation effects forbid the observation of most quantum effects in the motion of a crystalline electron. Laser cooling of atoms has brought a revival of interest in such problems, as it produces atoms whose de Broglie wavelength is comparable to the wavelength of the light interacting with the atoms, and whose resulting kinetic energy is comparable to the typical light shift induced by the radiation. The latter feature means that the cold atoms can be trapped in light potentials (or dipole potentials). The former means that the atom dynamics in such a potential is, in the absence of dissipation, essentially quantum. Moreover, the main source of dissipation is spontaneous emission, which can be arbitrarily reduced (if one has a powerful enough laser), while keeping a constant light potential just by an increase of the laser-atom detuning [3].

Light potentials are a consequence of the displacement of atomic levels resulting from the interaction with light, corresponding to a process in which a photon is absorbed, transferring the atom to an (virtual) excited state, from which the atom deexcites back to the ground state by *stimulated* emission. Such a process induces an energy shift of the atomic levels which can be deduced from second order perturbation theory and which is proportional to the light intensity, to the square of the coupling (that is, to $|\mathbf{d}_{eg} \cdot \boldsymbol{\epsilon}|^2$, where \mathbf{d}_{eg} is the dipole matrix element between the states g and e , and $\boldsymbol{\epsilon}$ is the polarization vector of the light), and to the inverse of the laser-atom detuning $\delta_L = \omega_L - \omega_{eg}$ (ω_{eg} is the Bohr frequency between states g and e). Any spatial gradient of this energy shift produces a (conservative) force, and thus a potential. A simple example is that of the standing wave formed by two counterpropagating, parallel-polarized beams. Placed

in such a standing wave, an atom perceives a periodic one-dimensional potential whose strength varies sinusoidally in the space. Standing waves (with small variations) form the model potential considered in the present work.

Light potentials generated by standing waves have been used in many experimental studies of quantum dynamics. For example, Bloch oscillations have been observed both with single atoms [4] and with a Bose-Einstein condensate [5] in an accelerated standing wave. Wannier-Stark ladders [6] and collective tunneling effects [7] have also been studied with such a system. Atoms placed in an intense, phase-modulated or pulsed standing wave realize a paradigmatic system for theoretical and experimental studies of quantum chaos, the so-called quantum kicked rotor [8–11].

In this paper, we consider the quantum dynamics of an atom (of mass M) placed in a tilted sinusoidal potential whose phase (that is, the position of its nodes) can be modulated in an arbitrary way, corresponding to the Hamiltonian

$$H = \frac{p^2}{2M} + v_0 \cos\{2k_L[x - x_0(t)]\} + f(t)x, \quad (1)$$

where $2k_L x_0(t)$ is a phase and $f(t)$ a force, both being (eventually) time dependent, and $k_L = 2\pi/\lambda_L$ is the wave number of the laser beam forming the standing wave. Different temporal dependences of $x_0(t)$ can be considered. For instance, the accelerated case $x_0(t) = (1/2)at^2$, which was studied in [4–7], is equivalent to an inertial force $F = Ma$ in the frame of the potential (see the Appendix).

A natural energy unit in such a context is the “recoil energy,” defined as the change in kinetic energy of the atom corresponding to the absorption of a photon, given by

$$E_R = \frac{\hbar^2 k_L^2}{2M}, \quad (2)$$

with which one can associate a recoil frequency $\omega_R = E_R/\hbar$ and a recoil momentum $p_R = \hbar k_L$, etc. It is also useful to rescale the variables: $X \equiv x/(\lambda_L/2)$, where $\lambda_L/2$ is the step of the periodic lattice, and $\tau \equiv \omega_R t$. With these definitions, the above Hamiltonian takes the following form, which is retained in the rest of the paper:

*Electronic address: quentin.thommen@univ-lille1.fr

[†]Electronic address: jean-claude.garreau@univ-lille1.fr

[‡]Electronic address: veronique.zehnle@univ-lille1.fr

[§]URL: <http://www.phlam.univ-lille1.fr>

$$H = \frac{p^2}{2m^*} + V_0 \cos\{2\pi[X - X_0(\tau)]\} + F(\tau)X, \quad (3)$$

where $V_0 \equiv v_0/E_R$ and $F \equiv f\lambda_L/2E_R$ [note that in this system the momentum operator in the real space is $P = -i(\partial/\partial X)$, $\hbar = 1$, the reduced mass is $m^* = \pi^2/2$, and $d = 1$ is the step of the lattice]. For simplicity, in what follows, we shall write the rescaled variables x , p , and t .

In the next section, we briefly review the time-independent Hamiltonian case in Eq. (3), introduce the Wannier-Stark basis, and show that it leads to a very simple description of the Bloch oscillation. In the following sections, we shall discuss the more complicated dynamics that arises when a harmonic modulation of the lattice is applied.

II. THE BLOCH OSCILLATION IN THE WANNIER-STARK DESCRIPTION

Bloch oscillation (BO) is a well known phenomenon discovered by Zener while studying the quantum properties of an electron in a (perfect) crystal submitted to a constant electric field [2]. The BO arises when a small spatial tilt is added to the lattice: Quantum particles do not fall along the slope of the potential, but perform a periodic, bounded, oscillation. BO is thus a strictly quantum behavior. We shall call the untilted potential the “lattice,” and the sum of the lattice and the tilted potential the “tilted lattice.”

The BO is usually described in the basis of the so-called *Bloch states* [1], i.e., the eigenstates of the lattice. In this paper, we use another framework corresponding to the eigenstates of the tilted potential. While the lattice is invariant under spatial translations by a multiple of the spatial period d , the tilted lattice has a more complicated symmetry: it is invariant under simultaneous spatial translation by a lattice period d and energy translation by $\omega_B = Fd$ (ω_B is the “Bloch frequency”). One then expects the eigenenergies to form “ladder” structures separated by ω_B , the so-called Wannier-Stark ladders, introduced by Wannier in connection with the problem of electrons in a crystal submitted to a homogeneous electric field [12]. Each element of the ladder corresponds to eigenfunctions (the Wannier-Stark states) centered at a given well, and thus separated by an integer multiple of d . The form and even the existence of these eigenstates has been the object of a long controversy, that was settled only recently [13]. In the present paper, we consider a spatially limited lattice, extending over many periods, and limited by an infinite-height box. This changes only very slightly the “bulk” properties of the system, and the eigenenergies and eigenstates obtained numerically display (to a very good approximation) the expected ladder structure described above. In this framework, the Wannier-Stark states (WSS's) are the eigenfunctions of the system. The relation to the case of an infinite tilted lattice is no problem if the corresponding states (Wannier-Stark resonances) have long enough lifetimes compared to the experimental times. The existence of these states was evidenced in 1988 in a semiconductor superlattice [14], and in 1996 with cold atoms in an optical lattice [6]. Note that, being spatially localized,

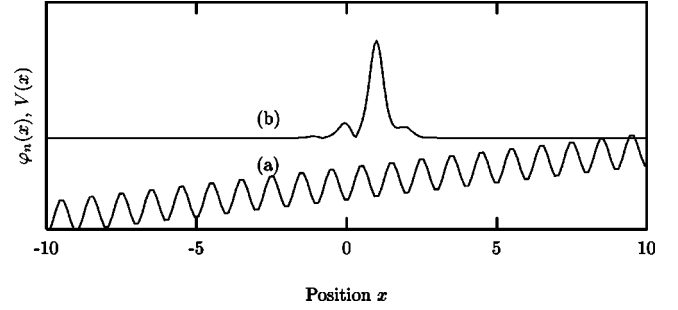


FIG. 1. (a) Periodic potential with a tilt. (b) The WSS state φ_n is localized in the well of index $n = 1$ and has appreciable overlap with neighbor lattice sites $n = 0, 2$. This eigenfunction is obtained for $V_0 = 2.5$ and $F = 0.5$. The “numerical” box includes 64 lattice sites.

Wannier-Stark states provide an ideal tool for the description of the wave function of a cold atom [as produced by a “Sisyphus-boosted” magneto-optical trap (MOT)] placed in the potential, whose de Broglie wavelength (around $\lambda_L/3$) is of the order of the lattice period $\lambda_L/2$.

Consider the properties of the time-independent Hamiltonian H_0 ,

$$H_0 = \frac{p^2}{2m^*} + V_0 \cos(2\pi x) + Fx, \quad (4)$$

where F is a constant force. The eigenfunctions of H_0 are Wannier-Stark states forming an energy ladder whose separation is $\omega_B = Fd$, $E_{nm} = E_m + nFd$.

The BO can be advantageously described by using the Wannier-Stark state localized inside a given individual lattice well, corresponding to the lowest energy of the states associated with this well (see Fig. 1). Note that considering only the ground state of each well is equivalent to a restriction to the first Bloch band in the description based on Bloch states. We also choose strong enough F and V_0 to produce well-localized WSS's [15]. The WSS associated with the lattice well labeled n is denoted $\varphi_n(x)$ (supposed real) and the corresponding eigenenergy is E_n (we drop the index m). The symmetries of the potential discussed above then imply

$$\varphi_{n+p}(x) = \varphi_n(x - pd) \quad (5)$$

and

$$E_{n+p} = E_n + pFd. \quad (6)$$

Let us describe the atomic wave function by a superposition of WSS's:

$$\Psi(x, t) = \sum_n c_n(t) \varphi_n(x) \quad (7)$$

with $c_n(t) = c_n e^{-iE_n t}$, c_n being the amplitude at $t = 0$. The dynamical quantities of the atom can be easily calculated. For instance, the mean value of the atomic position operator is

$$\langle x \rangle = \sum_n X_{n,n} |c_n|^2 + \sum_{n < m} (X_{n,m} c_n^* c_m e^{i(E_n - E_m)t} + \text{c.c.}), \quad (8)$$

where $X_{n,m} \equiv \langle \varphi_n | x | \varphi_m \rangle$. As long as the WSS φ_n is well localized in the respective well, we can keep only nearest-neighbor contributions ($n = m \pm 1$) and derive a simplified expression:

$$\langle x \rangle = \bar{x} + X_{n,n+1} \left(\sum_n c_n^* c_{n+1} e^{-i\omega_B t} + \text{c.c.} \right), \quad (9)$$

where $\bar{x} = \sum X_{n,n} |c_n|^2$ is the mean position of the wave packet and $X_{n,n+1} = X_{0,1} = X_{0,-1} = X_{n,n-1}$ is independent of n [16]. This result evidences a counterintuitive property of the quantum motion in a tilted lattice: instead of falling along the slope, the atom performs an oscillation with frequency ω_B (the Bloch frequency). The amplitude of this Bloch oscillation is proportional to $X_{0,1}$ and grows with the overlap between neighbor WSS's, i.e., for a small slope F and small lattice depth V_0 . The physical origin of the BO appears here clearly as an interference effect between neighbor sites, as $c_n^* c_{n+1}$ is the coherence between the sites n and $n+1$. Note the lack of oscillations if the atom is localized in only one well. Equation (8) also predicts the occurrence of harmonics with frequency $p\omega_B$ (p integer) but with smaller amplitudes since they involve the coupling strength $X_{n,n+p}$ [17].

The description of the BO given here is very different from the usual ‘‘solid-state’’ approach. There, the Bloch states (eigenstates of the untilted lattice) are taken as the reference basis. The oscillation is described in a semiclassical frame as the periodic evolution of the atom's quasimomentum Ft (in the first Brillouin zone) with period $T = 2\pi/(Fd)$ [18,19]. Although natural, this approach does not make clear the role of quantum interference produced by the periodic lattice structure as the basic mechanism underlying the Bloch oscillation, which is evidenced in our approach.

III. THE MODULATED POTENTIAL IN THE WANNIER-STARK DESCRIPTION: RESONANT DYNAMICS

With the existence of the natural frequency ω_B of the system in mind, one is tempted to investigate the quantum dynamics in the presence of a harmonic external forcing. The WSS approach proves to be very efficient, since it allows a fully analytical description. After some general considerations, we study in this section the case of resonant forcing, and show that it leads to a very rich and interesting dynamics. The general (nonresonant) case will be treated in the next section.

Consider the Hamiltonian of Eq. (3) with a constant force F and a lattice phase modulation

$$x_0(t) = a \sin(\omega t). \quad (10)$$

The developments are simpler if we use a unitary transformation that transforms the modulation into a time-dependent force. Physically, this is equivalent to moving to an accelerated reference frame in which the lattice is at rest [4,21],

adding thus an inertial force (see the Appendix). In this frame, the new Hamiltonian is given by Eq. (4) plus a time-dependent force $F'(t)$:

$$\begin{aligned} F'(t) &= m^* \frac{d^2 x_0(t)}{dt^2} = -m^* a \omega^2 \sin(\omega t) \\ &= -F_0 \sin(\omega t), \end{aligned} \quad (11)$$

where $F_0 \equiv m^* a \omega^2$ is the amplitude of the inertial force. The harmonic time dependence in Eq. (11) is the analog of an electric field for electrons in a (perfect) crystal. The dynamics in such a system can be described in a quite simple fashion by writing the state of the atom as a superposition of WSS's, Eq. (7). The coefficients $c_n(t)$ can be obtained by substituting Eq. (7) in the Schrödinger equation

$$[H_0 - F_0 x \sin(\omega t)] \Psi(x, t) = i \frac{\partial \Psi(x, t)}{\partial t}, \quad (12)$$

where H_0 is given by Eq. (4), with eigenstates $\varphi_n(x)$. This produces the following set of coupled differential equations for the $c_n(t)$:

$$\dot{c}_n(t) = -iE_n c_n(t) + iF_0 \sin(\omega t) \sum_m X_{n,m} c_m(t), \quad (13)$$

where $\dot{c}_n \equiv dc_n/dt$. Neglecting temporarily the coupling between different WSS's (i.e., putting $X_{n,m} = X_{n,n} \delta_{m,n}$), the amplitudes are obtained simply as $c_n = \exp[i\phi_n(t)]$, with the time-dependent phase

$$\phi_n(t) = -E_n t - \frac{F_0 X_{n,n}}{\omega} \cos(\omega t), \quad (14)$$

where $X_{n,n} = X_{0,0} + nd$ depends on the site index n [16]. We now write $c_n(t) \equiv d_n(t) e^{i\phi_n(t)}$. The amplitudes d_n obey the following system of differential equations:

$$\begin{aligned} \dot{d}_n &= iF_0 \sum_{m \neq n} X_{n,m} d_m(t) \exp[i(\phi_m(t) - \phi_n(t))] \\ &\quad \times \sin(\omega t). \end{aligned} \quad (15)$$

After Eq. (14), the phase difference $\phi_m(t) - \phi_n(t)$ is

$$\phi_m(t) - \phi_n(t) = (n-m) \left[\omega_B t + \frac{F_0 d}{\omega} \cos(\omega t) \right], \quad (16)$$

where we used Eq. (6). Equation (15) can be recast as

$$\begin{aligned} \dot{d}_n &= iF_0 \sum_{p \neq 0} X_p d_{n+p} [e^{-ip\omega_B t} e^{-i(pF_0 d/\omega) \cos(\omega t)}] \\ &\quad \times \sin(\omega t) \end{aligned} \quad (17a)$$

$$\begin{aligned} &= \frac{F_0}{2} \sum_{p \neq 0} X_p d_{n+p} \sum_l (-i)^l J_l \left(p \frac{F_0 d}{\omega} \right) \\ &\quad \times \{ e^{i[(l+1)\omega - p\omega_B]t} - e^{i[(l-1)\omega - p\omega_B]t} \}, \end{aligned} \quad (17b)$$

where $X_p \equiv X_{n,n+p}$ [16]. $J_n(x)$ is the Bessel function of the first kind, and we have used the well-known property of Bessel functions:

$$e^{-iz \cos(\omega t)} = \sum_{l=-\infty}^{+\infty} J_l(z) (-i)^l e^{il\omega t}. \quad (18)$$

Note that the sum over lattice sites (i.e., over p) extends over only a few neighboring sites, since the coupling coefficients X_p rapidly shrink to zero [17]. If the modulation is smooth enough to avoid projections on other states of the system, the sum over the harmonics of the modulation (i.e., l) is also limited to a few terms close to $l=0$ [typically, $l_{max} \sim pF_0d/\omega = pm^*a\omega d \sim O(1)$]. Therefore, only a finite number of terms are to be retained in the above expression. On the other hand, the evolution of d_n described by Eq. (17b) is a sum of oscillations with frequencies $[(l \pm 1)\omega - p\omega_B]$. In the following we keep only the so-called *secular* terms, that is, terms that oscillate slowly or do not oscillate at all. The resulting “close to resonance” dynamics is observed when $(l \pm 1)\omega \approx p\omega_B$, i.e., when the forcing frequency ω is commensurable (or almost) with the system’s natural frequency ω_B .

Let us consider the simpler resonant case $\omega = \omega_B$. Due to the relative strength of the factors X_p we can keep, to a good accuracy, only the contribution of the next-neighbor site ($p = 1$), which leads to the following expression:

$$\dot{d}_n(t) = \Omega_1 [d_{n+1} - d_{n-1}], \quad (19)$$

where

$$\begin{aligned} \Omega_1 &= \frac{F_0 X_1}{2} \left[J_0 \left(\frac{F_0 d}{\omega_B} \right) + J_2 \left(\frac{F_0 d}{\omega_B} \right) \right] \\ &= \frac{\omega_B X_1}{d} J_1 \left(\frac{F_0 d}{\omega_B} \right). \end{aligned} \quad (20)$$

This equation is similar to a “dipole coupling” between sites n and $n \pm 1$, where Ω_1 plays the role of a Rabi frequency. Note that, contrary to intuition, the coupling toward the left or toward the right neighbor is the same.

The meaning of Eq. (19) can be better appreciated by searching for plane-wave solutions of the form

$$d_n(t) = e^{i(k_0 d n + \omega t)}. \quad (21)$$

The (dimensionless) wave number k_0 takes into account the phase difference between neighbor sites. Substitution into Eq. (19) leads to the dispersion relation

$$\omega = 2\Omega_1 \sin(k_0 d) \quad (22)$$

and to the group velocity $v_g \equiv d\omega/dk_0$:

$$v_g = 2\Omega_1 d \cos(k_0 d). \quad (23)$$

This result shows that the dynamics is different depending on the wave number k_0 . For instance, if $k_0 d = \pm \pi/2$ (phase quadrature from site to site), $v_g = 0$ and there is no global

motion. If $k_0 d = \pi$, $v_g = -2\Omega_1 d$ and the global motion is a fall along the slope of the potential with the maximum speed $2\Omega_1 d$. More interesting is the case $k_0 = 0$, where $v_g = 2\Omega_1 d$: the atom then climbs up the slope of the potential with a constant maximum speed; there is, in this case, *coherent transfer of energy* from the modulation to the atom, thanks to the particular phase relations between neighboring sites. Note also that, contrary to the motion of a classical particle, the speed $|v_g|$ is independent of the sense of the motion: the wave packet climbs the slope up or down at the same speed.

More detailed information on the wave packet motion can be obtained by writing the amplitude d_n in the more general form

$$d_n(t) = f_n(t) e^{i(k_0 d n + \omega t)}, \quad (24)$$

where f_n are complex amplitudes describing the envelope of the atomic wave packet, assumed to vary slowly in time as compared to the frequency ω_B , and in space as compared to the lattice period d . Substituting the above expression into Eq. (19), we get

$$\begin{aligned} \dot{f}_n + i\omega f_n &= \Omega_1 (\cos(k_0 d)(f_{n+1} - f_{n-1}) \\ &+ i \sin(k_0 d)(f_{n+1} + f_{n-1})). \end{aligned} \quad (25)$$

Using the dispersion relation Eq. (22) and keeping only slowly varying contributions, we obtain

$$\begin{aligned} \dot{f}_n &= \Omega_1 (\cos(k_0 d)(f_{n+1} - f_{n-1}) \\ &+ i \sin(k_0 d)(f_{n+1} + f_{n-1} - 2f_n)). \end{aligned} \quad (26)$$

Since f_n vary slowly in space, we can take the continuous limit (with respect to the variable $x = nd$) and deduce the following equation for the wave packet envelope:

$$\dot{f}(x, t) = \Omega_1 \left(2d \cos(k_0 d) \frac{\partial}{\partial x} + id^2 \sin(k_0 d) \frac{\partial^2}{\partial x^2} \right) f(x, t). \quad (27)$$

This equation is an interesting piece of information. If $k_0 d = \pm \pi/2$, one has a diffraction equation of the form $\dot{f} = \pm i\Omega_1 d^2 \partial_x^2 f$, which describes the spreading of the atomic wave packet (i.e., diffraction) with no global displacement. The case $k_0 d = 0, \pi$ gives the wave equation $\dot{f} = v_g \partial_x f$ ($v_g = 2d\Omega_1$), describing a wave packet traveling with constant velocity v_g and no deformation: the wave packet presents an ascending or descending coherent motion. Mixed behaviors, i.e., spreading at a diffusion rate $\Omega_1 d^2 \sin(k_0 d)$ and uniform displacement with group velocity $v_g = 2\Omega_1 d \cos(k_0 d)$, are found for other values of k_0 . The general solution can easily be obtained by performing a spatial Fourier transform of Eq. (27).

The above result shows that, depending on the initial wave number k_0 , i.e., on the way the initial wave packet is prepared, the atom behaves in qualitatively different ways. Figures 2 and 3 are obtained by a direct integration of the Schrödinger equation, with the Hamiltonian given by Eq.

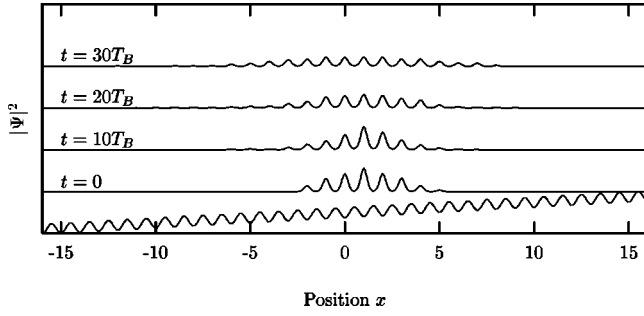


FIG. 2. The motion of the wave packet is obtained from a full integration of the Schrödinger equation corresponding to the modulated tilted lattice. The wave packet at $t=0$ has a site-to-site phase of $\pi/2$. The wave packet spreads in time with no displacement, in agreement with the theoretical prediction. Parameters are $V_0=2.5$, $F=0.5$, $\omega=\omega_B=0.5$, and $a=0.2$.

(12), for different evolution times. In the first case the initial wave packet is prepared with site-to-site phase $k_0d = \pi/2$ and diffraction is clearly visible, as predicted. In Fig. 3, the wave packet, prepared with $k_0=0$, has a uniform displacement while preserving its shape. Its group velocity obtained from the numerical simulations is $v_g=0.030$, in very good agreement with the theoretical value from Eq. (23), which is $v_g=0.032$.

Other resonant behaviors are observed if $\omega=q\omega_B$ (q integer). From the general expression of Eq. (17), one finds for instance a next-to-neighbor ($n \rightarrow n \pm 2$) resonant interaction if $\omega=2\omega_B$, leading to

$$\dot{d}_n(t) = \Omega_2[d_{n+2} - d_{n-2}] \quad (28)$$

with $\Omega_2 = (\omega_B/d)X_2J_1(F_0d/\omega_B)$. Note that $X_2 \ll X_1$ [17]. We illustrate in Fig. 4 the temporal evolution of a wave packet, obtained by numerical integration of the Schrödinger equation. The initial state is prepared as a superposition of two packets: one packet is constructed with in-phase amplitudes (that is, c_n and c_{n+2} have the same phase for n odd), and the other one is constructed with amplitudes in phase opposition (that is, c_n and c_{n+2} have opposite signs for n even). The first packet moves with velocity $v_g=4\Omega_2d$, and the second with $v_g=-4\Omega_2d$. The figure displays an original

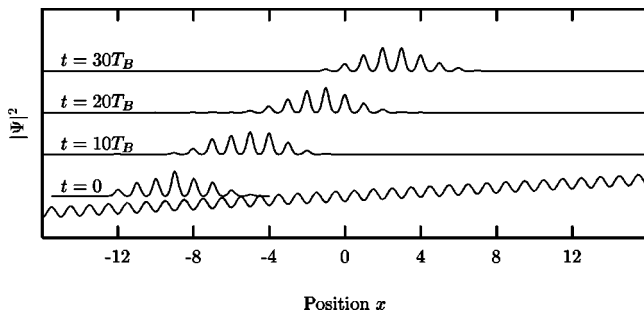


FIG. 3. Same as Fig. 2, except that the site-to-site phase is $k_0=0$. The wave packet has a shape-preserving motion up the slope of the potential. The observed group velocity is 0.030, in good agreement with the prediction of Eq. (23), $v_g=0.032$ ($X_{0,1}=0.13$).

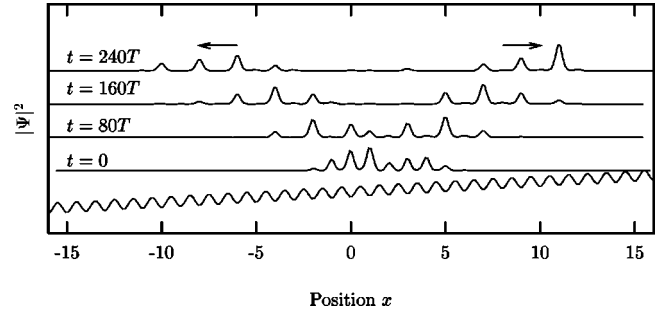


FIG. 4. Evolution of a wave packet for $\omega=2\omega_B$. The initial wave packet is a superposition of φ_n (n odd) which are in phase, and of φ_n (n even) with phase difference π . The initial wave packet separates into two packets with opposite velocities.

behavior showing each of these two initially interpenetrated packets moving independently in opposite directions, creating a highly delocalized state.

IV. THE MODULATED POTENTIAL: GENERAL CASE

In this section we generalize the results of the preceding section to the case of a nonresonant modulation. We follow essentially the same steps as in Sec. III, and we shall skip algebraic details of the calculations. Coming back to Eq. (17a) and looking for a solution of the form

$$d_n(t) = e^{i(k_0dn + \phi(t))}, \quad (29)$$

one gets the instantaneous frequency

$$\dot{\phi} = 2F_0 \sum_{p>0} X_p \cos\{p[k_0d - \theta(t)]\} \sin(\omega t), \quad (30)$$

where $\theta(t) = \omega_B t + (F_0d/\omega)\cos(\omega t)$, and we used $X_p = X_{-p}$. The group velocity $v_g = d\dot{\phi}/dk_0$ is thus

$$v_g = 2F_0d \sum_{p>0} pX_p \sin\{p[\theta(t) - k_0d]\} \sin(\omega t). \quad (31)$$

As in the preceding section, more detailed behavior is obtained by putting

$$d_n(t) = f_n(t) e^{i(k_0dn + \phi(t))}, \quad (32)$$

where f_n are slowly varying amplitudes. The generalization of Eq. (26) is then

$$\dot{f}_n = iF_0 \sum_{p \neq 0} X_p [f_{n+p} - f_n] e^{ip(k_0d - \theta)} \sin(\omega t) \quad (33)$$

or

$$\begin{aligned} \dot{f}_n = F_0 \sum_{p>0} X_p \sin(\omega t) & (-[f_{n+p} - f_{n-p}] \sin[p(k_0d - \theta)] \\ & + i[(f_{n+p} + f_{n-p} - 2f_n)] \cos[p(k_0d - \theta)]). \end{aligned} \quad (34)$$

Taking the continuous limit of the above expression then produces an equation describing both the propagation and the diffraction of the wave packet:

$$\begin{aligned} \dot{f}(x,t) = & \left(v_g(t) \frac{\partial}{\partial x} + iD(t) \frac{\partial^2}{\partial x^2} \right) f(x,t) \\ & + 2iF_0 \sum_{p \geq 2} X_p \cos[p(\theta - k_0 d)] \\ & \times \sin(\omega t) f(x,t), \end{aligned} \quad (35)$$

where

$$D(t) = F_0 d^2 \sum_{p > 0} p^2 X_p \cos[p(\theta - k_0 d)] \sin(\omega t) \quad (36)$$

and the group velocity v_g is given by Eq. (31). Note that the last term in Eq. (35) is a phase term which is $O(X_2) \ll 1$ and does not contribute to the probability density $|f(x,t)|^2$. For the sake of brevity, it is not considered in the following.

The Fourier transform of Eq. (35) with respect to x produces an algebraic equation for the Fourier transform $\tilde{f}(k,t)$ of $f(x,t)$, whose solution is

$$\tilde{f}(k,t) = e^{ikx'(t)} e^{ik^2 \Delta(t)} \tilde{f}(k,0) \quad (37)$$

and thus

$$f(x,t) = \frac{1}{\sqrt{2\pi}} \int e^{ik[x+x'(t)]} e^{ik^2 \Delta(t)} \tilde{f}(k,0) \quad (38)$$

with

$$x'(t) = \int_0^t v_g(\tau) d\tau \quad (39)$$

and

$$\Delta(t) = \int_0^t D(\tau) d\tau. \quad (40)$$

These expressions describe a coherent motion of the wave packet formed by an oscillatory motion with the time-dependent group velocity Eq. (31), and a diffusive motion with a time-dependent diffusion coefficient $D(t)$. For example, if one builds an initial Gaussian packet of width a_0 , $f(x,0) = \exp(-x^2/a_0^2)$, one finds, after some straightforward calculations,

$$|f(x,t)|^2 = \frac{a_0}{a(t)} \exp\left(-\frac{2x(t)^2}{a(t)^2}\right), \quad (41)$$

where

$$a(t) = a_0 \left[1 + 16 \frac{\Delta(t)^2}{a_0^4} \right]^{1/2}. \quad (42)$$

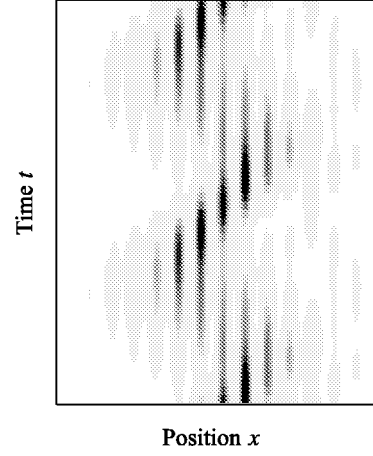


FIG. 5. Spatiotemporal behavior of $|\Psi(x,t)|^2$ obtained numerically by integration of the Schrödinger equation (gray level convention: the maximum values of $|\Psi(x,t)|^2$ are depicted in black), from $t=0$ to $t=4\pi/\delta$ (that is, two periods of the beat frequency $\delta = \omega - \omega_B = 0.02$). Other parameters are the same as in Fig. 2.

The physical meaning of our development can be evidenced by considering the case where ω differs from ω_B by a small detuning $\delta = \omega - \omega_B$, $|\delta| \ll \omega_B$, and keeping only leading-order terms of order $O(\delta^{-1})$. The wave packet then undergoes a harmonic oscillation at the beat frequency δ with a group velocity given by Eq. (31):

$$v_g(t) = 2\Omega_1 d \cos(k_0 d + \delta t), \quad (43)$$

corresponding to a periodic mean position displacement

$$\langle x(t) \rangle = x(0) - \frac{2\Omega_1 d}{\delta} [\sin(k_0 d + \delta t) - \sin(k_0 d)]. \quad (44)$$

The width of the wave packet oscillates in a breathing mode which is governed by

$$\Delta(t) = \frac{\Omega_1 d^2}{\delta} [\cos(k_0 d + \delta t) - \cos(k_0 d)]. \quad (45)$$

The results of Sec. III for a resonant excitation are naturally recovered in the limit $\delta \rightarrow 0$.

We have performed the integration of the Schrödinger equation for a detuning $\delta = 0.02$. Figure 5 shows the spatiotemporal dynamics of the wave packet and clearly evidences the periodic oscillations and the breathing at frequency δ predicted above. Figure 6 shows the mean position and width of the wave packet as a function of time. The comparison with the theory is very good. For instance, the amplitude of $\langle x(t) \rangle$ is found numerically as 1.55 compared to the theoretical value 1.73.

V. CONCLUSION

We have studied, in a fully analytical way, the dynamics of a wave packet in a static and time-modulated tilted potential in the framework of the Wannier-Stark states. This basis is well suited to the description of the state of a cold atom (as

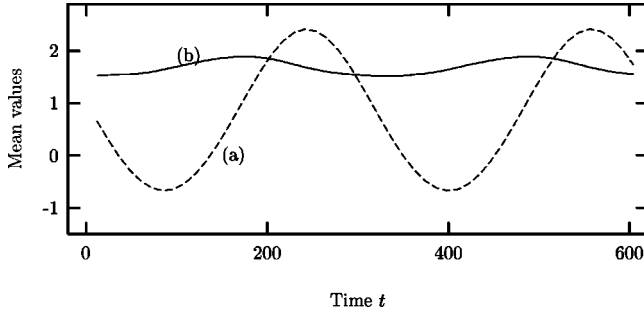


FIG. 6. Mean values (a) $\langle x(t) \rangle$ and (b) $\sqrt{\langle x^2(t) \rangle - \langle x(t) \rangle^2}$ obtained from the wave packet dynamics depicted in Fig. 5.

produced by a Sisyphus-boosted MOT). Moreover, it provides a simple description the atomic dynamics, which has been proved to be very rich: A variety of coherent motions is obtained depending on the preparation of the initial wave packet and its site-to-site quantum coherence. We can also note that the description introduced here is, in principle, independent of the details of the lattice, provided it presents localized states in the lattice sites. It is therefore generalizable to other kinds of lattice.

Note that the present work is distinguished from the more usual “solid-state” approach, which is based on Bloch functions. We postpone for a forthcoming work a detailed comparison between the Wannier-Stark and Bloch approaches.

Finally, let us discuss the possibility of experimental observations in cold atom systems. The experimental difficulties are fourfold: the creation of site-to-site atomic coherence, suppression of dissipative effects, limited interaction time between the atoms and the potential, and detection of the atom’s dynamics.

As we have seen in Sec. II, all coherent motion ultimately depends on the site-to-site atomic coherence $c_n c_{n+1}^*$. There are various ways of creating this kind of coherence. The most usual is Raman cooling, which consist in previous sub-recoil cooling of the atoms so that their de Broglie wavelength is of the order of a few lattice steps (five lattice steps is typical) [4]; the light potential is then turned on adiabatically. Another way of creating spatial coherence is to start with a Bose-Einstein condensate, whose spatial coherence length is up to hundreds of lattice sites [5,7]. Note that in the latter case the system obeys a nonlinear Schrödinger equation, and the approach described above may not apply.

Dissipation, in the present context, is due to spontaneous emission (see Sec. I). The usual lasers, working on wavelengths corresponding to alkali-metal atoms, allow one to work at detunings corresponding to about 10^3 – 10^4 times the natural width of the transition concerned, which means that spontaneous emission is limited to less than one photon per second. As the characteristic time of the system, the Bloch period, is typically 100 μ s, the observation of the effects discussed here is therefore not limited by dissipation. The transit time in the laser beams creating the potential is a more

serious problem, as the atoms are confined only in one dimension by the potential. If these beams are horizontal, the atoms are free falling. The interaction time is of the order of 10 ms and typically 100 times greater than the Bloch period.

The detection of the coherent dynamics described above is simpler in *momentum* space, thanks to the possibility of using velocity-sensitive Raman stimulated transitions [4,20]. The coherent motion of atoms, e.g., when they climb the slope of the modulated potential (Sec. III), corresponds to a speed of about the recoil velocity, i.e., 3 mm/s for cesium. This is easily detectable by Raman stimulated spectroscopy. It would certainly be very interesting to also observe the coherent motion in real space. This seems to be very difficult, because the spatial amplitude of the motion is very small, of the order of a few lattice steps, as compared to the atomic cloud which extends over hundreds of lattice wells (for atoms cooled in a magneto-optical trap). The coherent dynamics is thus detectable in momentum space, but very hard to see in real space, at least under the usual experimental conditions.

ACKNOWLEDGMENTS

The authors acknowledge S. Bielański for fruitful discussions. Laboratoire de Physique des Lasers, Atomes et Molécules (PhLAM) is UMR 8523 du CNRS et de l’Université des Sciences et Technologies de Lille. Center d’Etudes et Recherches Lasers et Applications (CERLA) is supported by Ministère de la Recherche, Région Nord-Pas de Calais, and Fonds Européen de Développement Economique des Régions (FEDER).

APPENDIX: UNITARY TRANSFORMATION

Equation (11) is obtained if we perform the unitary transformation

$$U(t) = e^{iX_0(t)P} e^{-i\beta(t)X} e^{i\gamma(t)} \quad (\text{A1})$$

where we have included translation operators in space and momentum with $\beta = 2m^* \dot{X}_0$ (i.e., the momentum of a particle of mass m^*). In this framework, following [21], we obtain (with $UXU^\dagger = X + X_0$ and $UPU^\dagger = P + \beta$)

$$H' = UHU^\dagger + i(d_t U)U^\dagger = \frac{(P + \beta)^2}{2m^*} + V_0 \cos(2\pi X) \\ + F(X + X_0(t)) - \dot{X}_0(t)P + \dot{\beta}(t)(X + X_0) - \dot{\gamma}$$

with $\dot{\gamma} = FX_0 + m^* \dot{X}_0 X_0 + (m^*/2) \dot{X}_0^2$:

$$H' = \frac{p^2}{2m^*} + V_0 \cos(2\pi X) + [F + m^* \dot{X}_0(t)]X. \quad (\text{A2})$$

Therefore, in the frame of the periodic potential, the Hamiltonian contains an inertial force proportional to $\dot{X}_0(t)$.

- [1] F. Bloch, Z. Phys. **52**, 555 (1928).
- [2] C. Zener, Proc. R. Soc. London, Ser. A **145**, 523 (1934).
- [3] See, for example, *Fundamental Systems in Quantum Optics*, Proceedings of the Les Houches Summer School of Theoretical Physics, Session LIII, 1990, edited by J. Dalibard, J.M. Raimond, and J. Zinn-Justin (North-Holland, Amsterdam, 1992).
- [4] M. Ben Dahan, E. Peik, J. Reichel, Y. Castin, and C. Salomon, Phys. Rev. Lett. **76**, 4508 (1996).
- [5] O. Morsch, J.H. Müller, M. Cristiani, D. Ciampini, and E. Arimondo, Phys. Rev. Lett. **87**, 140402 (2001).
- [6] S.R. Wilkinson, C.F. Bharucha, K.W. Madison, Q. Niu, and M.G. Raizen, Phys. Rev. Lett. **76**, 4512 (1996).
- [7] B.P. Anderson and M. Kasevich, Science **282**, 1686 (1998).
- [8] F.L. Moore, J.C. Robinson, C.F. Bharucha, P.E. Williams, and M.G. Raizen, Phys. Rev. Lett. **73**, 2974 (1994); B.G. Klappauf, W.H. Oskay, D.A. Steck, and M.G. Raizen, *ibid.* **81**, 1203 (1998).
- [9] H. Amman, R. Gray, I. Shvarchuck, and N. Christensen, Phys. Rev. Lett. **80**, 4111 (1998).
- [10] J. Ringot, P. Szriftgiser, J.C. Garreau, and D. Delande, Phys. Rev. Lett. **85**, 2741 (2000).
- [11] M.B. D'Arcy, R.M. Godum, M.K. Oberthaler, M.K. Cassettari, and G.S. Summy, Phys. Rev. Lett. **87**, 074102 (2001).
- [12] G. Wannier, Rev. Mod. Phys. **62**, 645 (1962).
- [13] For a complete review of the subject, see G. Nenciu, Rev. Mod. Phys. **63**, 91 (1991).
- [14] J. Bleuse, G. Bastard, and P. Voisin, Phys. Rev. Lett. **60**, 220 (1988).
- [15] H. Fukuyama, R.A. Bari, and H.C. Fogdeby, Phys. Rev. B **8**, 5579 (1973).
- [16] By virtue of the translational properties of the WSS's, Eqs. (5) and (6), $X_{n,n+p}$ ($p \neq 0$) does not depend on n : $X_{n,n+p} = \int \varphi_n^*(x)x\varphi_{n+p}(x)dx = \int \varphi_0^*(x-nd)x\varphi_p(x-nd)dx = \int \varphi_0^*(x')(x'+nd)\varphi_p(x')dx' = X_{0,p}$, where we used the orthogonality of the WSS's. Note, however, that $X_{n,n} = X_{0,0} + nd$ does depend on n .
- [17] While the nearest neighbor interaction is proportional to $X_{0,1} = 0.13$, the next-to-neighbor interaction is $X_{0,2} = 7.8 \times 10^{-3}$, i.e., the amplitude of the oscillation at $2\omega_B$ is roughly 20 times smaller than that at ω_B (the numerical values were obtained for $F=0.5$ and $V_0=2.5$).
- [18] N.W. Ashcroft and N.D. Mermin, *Solid State Physics* (Holt, Rinehart and Winston, New York, 1976).
- [19] M. Holthaus, J. Opt. B: Quantum Semiclassical Opt. **2**, 589 (2000).
- [20] J. Ringot, P. Szriftgiser, and J.C. Garreau, Phys. Rev. A **65**, 013403 (2002).
- [21] M. Ben Dahan, thèse de doctorat, Université Paris VI, Paris, 1997.